KEY FINDINGS AND REMAINING QUESTIONS IN THE AREAS OF CORE-CONCRETE INTERACTION AND DEBRIS COOLABILITY

M. T. Farmer, S. Lomperski, C. Gerardi, and N. Bremer
Argonne National Laboratory
9700 S. Cass Avenue, Argonne, IL 60439, USA
farmer@anl.gov; lomperski@anl.gov; cgeradi@anl.gov; nbremer@anl.gov

S. Basu
U.S. Nuclear Regulatory Commission
MS-T10K8, 11545 Rockville Pike, Rockville, MD 20852, USA
Sudhamay.Basu@nrc.gov

ABSTRACT

The reactor accidents at Fukushima-Dai-ichi have rekindled interest in late phase severe accident behavior involving reactor pressure vessel breach and discharge of molten core melt into the containment. Two technical issues of interest in this area include core-concrete interaction and the extent to which the core debris may be quenched and rendered coolable by top flooding. The OECD-sponsored Melt Coolability and Concrete Interaction (MCCI) programs at Argonne National Laboratory included the conduct of large scale reactor material experiments and associated analysis with the objectives of resolving the ex-vessel debris coolability issue, and to address remaining uncertainties related to long-term two-dimensional molten core-concrete interactions under both wet and dry cavity conditions. These tests provided a broad database to support accident management planning, as well as the development and validation of models and codes that can be used to extrapolate the experiment results to plant conditions. This paper provides a high level overview of the key experiment results obtained during the program. A discussion is also provided that describes technical gaps that remain in this area, several of which have arisen based on the sequence of events and operator actions during Fukushima.

KEYWORDS
Core-concrete interaction, debris coolability

1. INTRODUCTION

1.1 Background

The reactor accidents at Fukushima-Dai-ichi have rekindled international interest in late phase severe accident behavior involving reactor pressure vessel breach and discharge of molten core material into the containment. Two technical issues of interest in this area include core-concrete interaction (CCI) and the extent to which the core debris may be quenched and rendered coolable by top flooding. The OECD-sponsored Melt Coolability and Concrete Interaction (OECD/MCCI) programs at Argonne National Laboratory [1-3] included the conduct of 20 reactor material separate- and integral-effect tests and associated analysis with the objectives of resolving the ex-vessel debris coolability issue, and to address remaining uncertainties related to long-term two-dimensional CCI under both wet and dry cavity conditions. The testing also included experimental demonstration of several engineered systems for stabilizing ex-vessel core debris (i.e., core catchers). In general, these tests provided a broad database to

support accident management planning, as well as the development and validation of models and codes that can be used to extrapolate the experiment findings to plant conditions. The overall intent of this paper is to provide a high level overview of key results from these tests and to identify remaining issues that still need to be addressed.

A variety of related studies have been carried out in this area. Regarding dry cavity behavior, early transient high temperature steel simulant experiments were conducted by Powers et al. [4,5] at Sandia National Laboratories to identify basic phenomenology associated with CCI. These early transient tests were followed by sustained heating experiments using metallic melts at different power levels carried out by Copus et al. [6,7] and Tarbell et al. [8] at Sandia, as well as Alsmeyer et al. [9,10] at Karlsruhe Institute of Technology (KIT) in Germany. Recently, Sevón et al. at VTT in Finland [11] conducted transient metal tests focused on quantifying the ablation characteristics for hematite concrete, which is the type used as sacrificial material in the EPR reactor pit. In terms of reactor material testing, a series of 1-D experiments addressing thermal-hydraulic behavior and fission product release were conducted by Thompson et al. [12] and Fink et al. [13] at Argonne National Laboratory. In addition to these tests, several large scale 1-D core melt tests were carried out at Sandia under both transient [14] and sustained heating [15-17] conditions. Finally, 2-D CCI experiments under dry cavity conditions have been carried out at the VULCANO test facility at CEA in France [18,19]. Currently, the MOCKA test program at the Karlsruhe Institute of Technology [20] is investigating the interaction of a simulant oxide and metal melt in a stratified configuration interacting with concrete containing rebar.

In terms of wet cavity CCIs, low temperature simulant experiments have been conducted by Theofanous et al. [21] to identify phenomena associated with melt coolability. High temperature simulant experiments have also been conducted by Blose et al. [22,23] and Sdouz et al. [24] at Sandia, as well as Alsmeyer et al. [25] at KIT, to investigate coolability with concurrent concrete erosion. In terms of reactor material testing, the COTELS [26,27] and MACE [2] experiment programs have been carried out to investigate coolability mechanisms under prototypic MCCI conditions.

1.2 Objectives and Approach

The overall objectives of the OECD/MCCI test series (Table I) was to provide information on: i) lateral vs. axial power split during dry CCI, ii) integral debris coolability data following late phase flooding, and iii) data regarding the nature and extent of the cooling transient following breach of the crust formed at the melt-water interface. The experiment approach was to investigate the interaction of reactor material core melt with specially-designed 2-D concrete test sections. The initial phase of the tests was conducted under dry cavity conditions. After a predetermined time interval and/or ablation depth was reached, the cavities were flooded with water to obtain data on the coolability of core melt after CCI had progressed for some time. Tests CCI-1 through CCI-3 principally addressed the effect of concrete type on 2-D cavity erosion behavior and late phase debris coolability. Test CCI-4 expanded the parameter base by examining the influence of core melt composition on cavity erosion behavior and coolability. The specific objectives were to: i) increase the metal content of the melt to the highest practical level (in the test facility) to more accurately mock up a BWR core melt composition, and ii) modify the apparatus design to increase the duration of the dry CCI phase. Conversely, CCI-5 focused on examining the influence of melt pool aspect ratio on the radial/axial power split under dry cavity conditions. Finally, a single large scale integral test (CCI-6) was conducted to provide a database for validation of severe accident codes under conditions in which the cavity is flooded early.

The balance of this paper begins by providing details of the apparatus used for carrying out the tests. A high level review of key findings from the tests related to CCI and debris coolability is then provided. Based on these results, a summary of remaining knowledge gaps in these two areas is then provided.

Table I. Specifications for OECD/MCCI CCI Tests.

Parameter	Specifications for Test:					
	CCI-1	**CCI-2**	**CCI-3**	**CCI-4**	**CCI-5**	**CCI-6**
Corium	100 % oxidized PWR + 8 wt% SIL	100 % oxidized PWR + 8 wt% LCS	100 % oxidized PWR + 15 wt% SIL	78 % oxidized BWR with 7.7 wt % SS and 10 wt % LCS[b]	100 % oxidized PWR + 15 wt% SIL	100 % oxidized PWR + 6 wt% SIL
Concrete type[a]	SIL (U.S.-type)	LCS	SIL (EU-type)	LCS	SIL (EU-type)	SIL (EU-type)
Basemat cross-section	50 cm x 50 cm	50 cm x 50 cm	50 cm x 50 cm	50 cm x 40 cm	50 cm x 79 cm	70 cm x 70 cm
Initial melt mass (depth)	400 kg (25 cm)	400 kg (25 cm)	375 kg (25 cm)	300 kg (25 cm)	590 kg (25 cm)	900 kg (28 cm)
Test section sidewall construction	Electrode walls: Inert Non-electrode walls: concrete	Electrode walls: Inert Non-electrode walls: concrete	Electrode walls: Inert Non-electrode walls: concrete	Electrode walls: Inert Non-electrode walls: concrete	Electrode walls: Inert Non-electrode wall #1: concrete Non-electrode wall #2: Inert	Electrode walls: Inert Non-electrode walls: concrete
Lateral/Axial ablation limit	35/35 cm	35/35 cm	35/35 cm	45/42.5 cm	40/42.5 cm	32.5/24 cm
Initial melt temperature	1950 ºC	1880 ºC	1950 ºC	1850 ºC	1950 ºC	2100 ºC
DEH input prior to flooding	Constant @ 150 kW	Constant @ 120 kW	Constant @ 120 kW	Constant @ 95 kW	Constant @ 145 kW	Constant @ 210 kW
DEH input after	Constant voltage	Constant voltage	Constant voltage	Constant voltage	N/A	Constant voltage
Criteria for water addition	*Late flooding*: i) 5.5 hour dry phase, or ii) ablation reaches within 5 cm of limit	*Late flooding*: i) 5.5 hour dry phase, or ii) ablation reaches within 5 cm of limit	*Late flooding*: i) 5.5 hour dry phase, or ii) ablation reaches within 5 cm of limit	*Late flooding*: i) 7 hour dry phase, or ii) ablation reaches within 5 cm of limit	N /A	*Early flooding:* Cavity ablation reaches 2.5 cm
Test termination criteria	i) Melt temperature falls below the concrete solidus, ii) ablation is arrested, or the iii) maximum ablation depth is reached axially or radially					
Operational Summary	Pronounced lateral erosion in one wall	Symmetrical cavity erosion	Pronounced lateral erosion	Symmetrical cavity erosion; *bridge crust formed during dry CCI phase, so no melt-water contact*	Pronounced lateral erosion; *cavity not flooded due to offgas system plugging*	Limited cavity erosion and effective debris cooling

[a]SIL denotes siliceous concrete, LCS denotes limestone/common sand concrete.
[b]After erosion of concrete/metal inserts and at start of basemat ablation

2. TEST FACILITY

A total of six large scale tests were conducted; specifications are provided in Table I, while key facility features are illustrated in Fig. 1. The facility consisted of a test apparatus, a power supply for Direct Electrical Heating (DEH) of the corium, a water supply system, two steam condensation (quench) tanks, a ventilation system to filter and exhaust the reaction product gases, and a data acquisition system. The internal cross-section of the apparatus above the lower test section that contained the core melt measured 50 cm x 50 cm. The concrete crucible was located at the bottom of the test section (Fig. 2(a)). The cross-sectional area of the concrete basemat was varied in the test series to meet different objectives. Specifically, for CCI-1 to CCI-3 the initial basemat surface area measured 50 cm x 50 cm, requiring an initial core melt mass of ~400 kg to achieve the target melt depth of 25 cm. In CCI-4 the basemat area was reduced to 40 cm x 50 cm to provide more concrete sidewall thickness, and thereby prolong the duration of the dry cavity ablation phase. Test CCI-5 focused on examining the influence of melt pool aspect ratio on the radial/axial power split under dry cavity conditions. The approach was to modify the design to include a single concrete sidewall that would undergo ablation, with the opposing sidewall was made from refractory MgO to essentially create an adiabatic boundary condition. The initial distance between the sidewalls was also increased from 50 cm to 79 cm to maximize the aspect ratio at the start of the test. With the adiabatic boundary condition on one wall implying symmetry, the effective test section width was increased to 158 cm from the 50 cm baseline size. In CCI-6, the sidewall thickness was reduced to accommodate a larger 70 cm x 70 cm basemat, the objective being to minimize sidewall effects. This step required increasing the initial melt mass to 900 kg for this integral-effect, early cavity flooding experiment. These variations in basemat size and corresponding wall thickness had an impact on the maximum allowable ablation depths in the tests. The axial limit was nominally 35 cm, while the radial limit varied from 32.5 to 45 cm depending on the test configuration.

As shown in Fig. 2(b), the other two sidewalls of the apparatus that backed up the tungsten electrodes were made from refractory MgO. These walls were lined with either crushed UO_2 pellets or U_3O_8 powder to provide additional protection against attack by the corium. This method was found to be highly effective over the course of the test program, with no attack of the underlying MgO observed in any of the experiments.

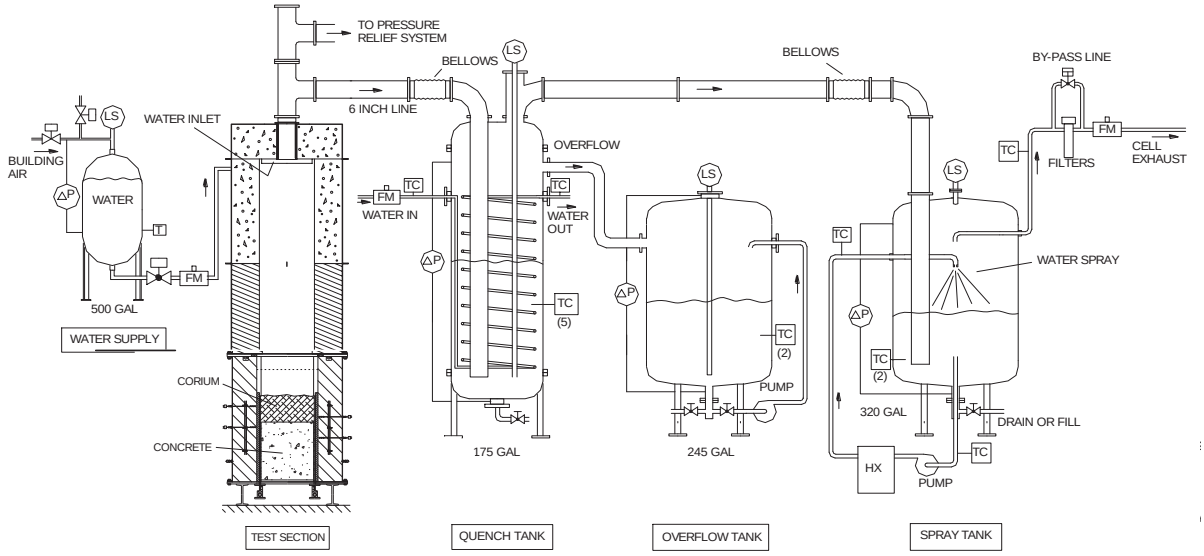

Figure 1. CCI Test Apparatus.

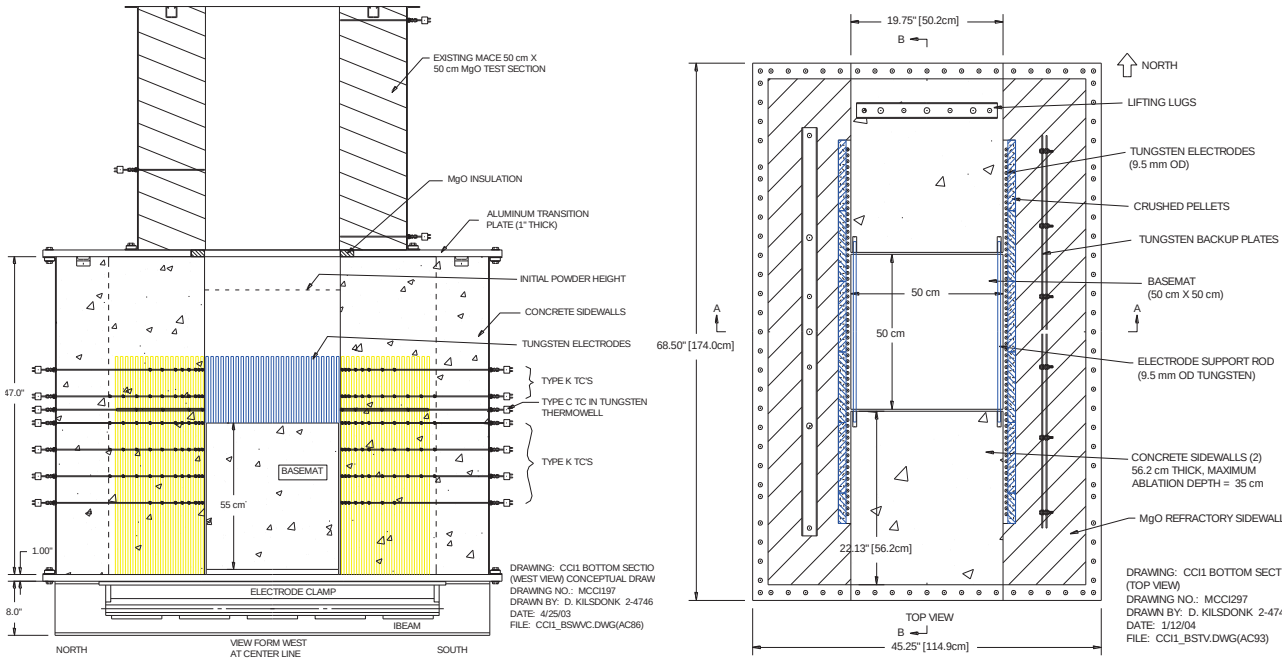

(a) **(b)**

Figure 2. (a) Side and (b) Top Views of Lower Test Section.

Melt generation for all tests was achieved through an exothermic chemical reaction yielding the target initial melt mass over a timescale of ~ 30 seconds. The melt compositions produced through these reactions are shown in Table I; see [1,3] for details regarding the experiment method. Test CCI-4 expanded the parameter base by examining the influence of core melt composition on cavity erosion behavior and coolability. The specific objective was to increase the metal content of the melt to the highest practical level (given the test facility constraints) to more accurately mock up a BWR core melt composition. This was achieved by placing a metal-bearing concrete insert on top of the concrete basemat that was ablated into the melt prior to onset of basemat ablation, thereby increasing the metal content to the target level.[1] After the chemical reaction, DEH was supplied to the melt to simulate decay heat through the two banks of tungsten electrodes. The electrodes were attached by water-cooled bus bars to a 560 kW AC power supply. The target input power was selected to match a typical heat flux to exterior surfaces of the melt zone during a typical reactor accident (i.e., ~ 200 kW/m^2 for CCI-1, and ~ 150 kW/m^2 for the other five tests) while accounting for parasitic heat losses to the MgO sidewalls. The gross input power levels selected to meet this objective are shown in Table I. During periods of dry cavity erosion, input power was held constant at the target value.

As shown in Fig. 1, a large gas line was used to vent the helium cover gas and the various gas species arising from the core-concrete interaction into two adjacent tanks that were partially filled with water. The cover gas and non-condensable gases (CO, CO_2, and H_2) passed through the tanks and were vented through an off-gas system that included a demister and filters. The gases were exhausted through the containment ventilation system and a series of high efficiency filters before being released from the building stack.

After a specified period of core-concrete interaction, the cavity was flooded using an instrumented water supply system. The water entered the test section through two weirs located in opposing (non-electrode)

[1]This technique was originally developed as part of the ACE/MCCI test series [12] that focused on quantifying fission product source term due to core-concrete interaction.

sidewalls at the top of the test section. For all tests, the cavity was flooded at a sufficient flowrate to ensure that the quench process would not be water-limited (i.e., 2 liters/sec, which corresponds to ~ 5 MW cooling rate assuming heat transfer occurs by boiling). Once a stable crust formed at the melt-water interface, a lance was used to breach the crust to obtain data on the nature and extent of debris cooling that occurs following transient crust breach. Based on counter-part crust strength tests carried out as part of the OECD/MCCI program [1,3], periodic breach is expected to occur at plant scale owing to the mechanical instability of crusts that would form in the large cavity span of most plants.

As noted in Table I, after cavity flooding the power supply operating procedure was switched from constant power to a constant voltage. This step was taken since the DEH method does not effectively heat solidified material formed as a result of the debris cooling process. Thus, operation in a constant voltage mode preserves the specific power density *in the melt zone*, which is the most prototypic method given the limitations of the DEH heating method.

The facility was instrumented to monitor and guide experiment operation and to log data for subsequent evaluation. Principal parameters monitored during the tests included the power supply voltage, current, and gross input power to the melt; melt temperature and temperatures within the concrete basemat and sidewalls; crust lance position and applied load; supply water flow rate; water volume and temperature within the test apparatus, and water volume and temperature within the quench system tanks. Other key data recorded by the DAS included temperatures within test section structural sidewalls, off gas temperature, and pressures at various locations within the system.

The concrete sidewalls and basemat were instrumented with multi-junction Type K thermocouple assemblies to determine the 2-D ablation profile as a function of time. In addition, several Type C thermocouple assemblies protected by tungsten thermowells were mounted vertically within the basemat and horizontally through the concrete sidewalls to provide data on the melt temperature distribution versus time. Other significant test instrumentation included a video camera for observing physical characteristics of the core-concrete interaction. Additional details regarding facility instrumentation are provided in [1,3].

3. RESULTS AND DISCUSSION

As a whole, the CCI test series investigated the effects of concrete type, melt composition, and input power on 2-D core-concrete interaction behavior under both wet and dry cavity conditions. The purpose of this section is to compare the results and identify key parametric effects. Principal variables either measured or inferred from the test results include melt temperature, local concrete ablation rates, and debris/water heat flux after cavity flooding. Posttest examinations were carried out to document the debris morphology, and chemical analysis was performed to determine the composition of various debris zones. All tests fully met their objectives except for CCI-4 and CCI-5. Although these tests provided valuable dry cavity ablation data, they provided no information on debris coolability. In CCI-4, direct melt-water contact was precluded by the presence of a large mantle crust that formed in the upper regions of the test section due to extensive melt foaming that occurred over the 6 hour period preceding cavity flooding. For CCI-5, the cavity was not flooded due to plugging of the main gas line for the apparatus at the beginning of the test; thus, there was a concern that the high steam production rate would over-pressurize the test section.

Figures 3-5 present key data from tests that provided information on dry cavity ablation, including the average melt temperature, characteristic lateral and axial concrete ablation rates. As shown in Fig. 3, the initial melt temperature for these tests was in the range of 1850-1950 ºC; differences were due to uncertainty-variability in the thermite reaction temperatures for the different chemical mixtures used to generate the initial melt compositions. During dry cavity operations, all tests showed the overall trend of

decreasing melt temperature as ablation progressed, which was due to a heat sink effect as relatively cool concrete slag was introduced into the melt, as well as the increasing heat transfer surface area as the melts expanded into the concrete crucibles. The decline in melt temperature may further reflect the evolution of the pool boundary freezing temperature that decreased as additional concrete was eroded into the melt over the course of the tests.

One of the objectives of the test series was to investigate the effect of unoxidized Zr cladding on the thermal-hydraulics of the CCI. To examine this effect, CCI-4 was conducted with a 78 % oxidized BWR melt composition (Table I). As is evident from Fig. 3, the effect of the oxidation reaction between Zr and sparging concrete decomposition gases (CO_2, H_2O) was to cause an exothermic transient in which the melt temperature increased by ~ 100 ºC during the first ~10 minutes of the test. This same type of transient was observed in metal tests conducted at Sandia [7-8] and KIT [10]. In addition, the effect of Zr oxidation was also investigated as part of the ACE/MCCI test series with core oxide material [12]. However, the tests in that series with partially oxidized cladding and LCS concrete were of very short duration (i.e., several minutes), and so the long term effects of the oxidation reactions on thermal-hydraulic behavior could not be discerned. However, CCI-4 ran for several hours past the point at which all the cladding had oxidized. Moreover, CCI-2 can be considered a counterpart experiment insofar as cladding oxidation state is concerned. Comparison of the results indicates that cladding oxidation reactions cause an early exothermic temperature transient in the melt, and after the reaction is complete, the temperature drops to that consistent with fully oxidized melt conditions.

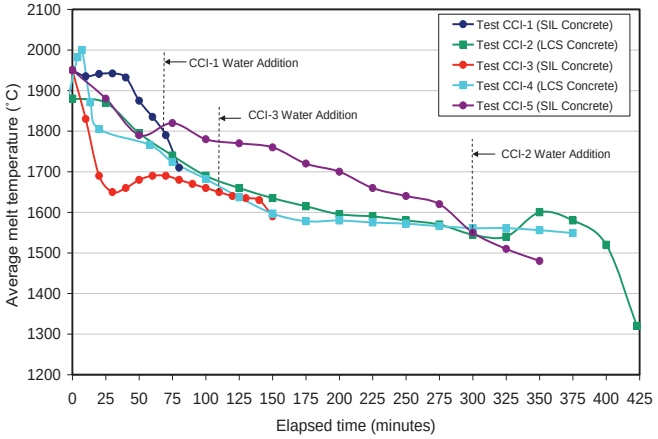

Figure 3. Melt Temperature for Late Flooding Tests.

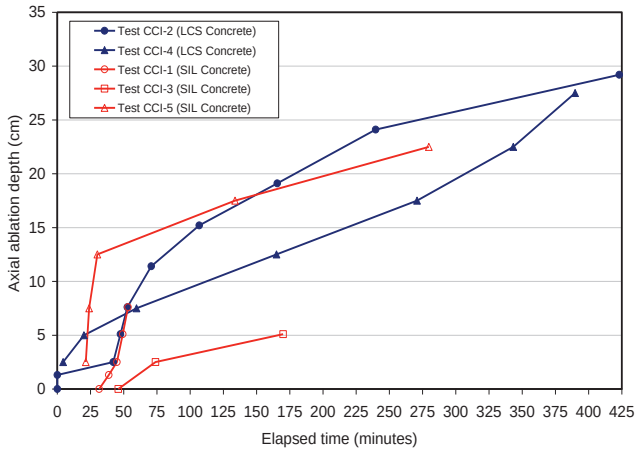

Figure 4. Axial Ablation for Late Flooding Tests.

Additional examination of Fig. 3 indicates that CCI-1 exhibited slightly different melt temperature behavior compared to the other fully oxidized tests. In this test, the melt temperature was relatively constant over the first ~40 minutes of the interaction. One possible contributor to this trend was the fact that CCI-1 was run at a 25 % higher power level in comparison to the other tests. In particular, CCI-1 was run at a level consistent with a heat flux of ~ 200 kW/m^2 over all surfaces initially in contact with the melt at the start of the experiment. Conversely, the other tests were initiated at a lower power level consistent with a flux of ~ 150 kW/m^2 (Table I). However, the lack of a temperature decline may have also been caused by crust formation at the core-concrete interfaces that acted to insulate the melt.

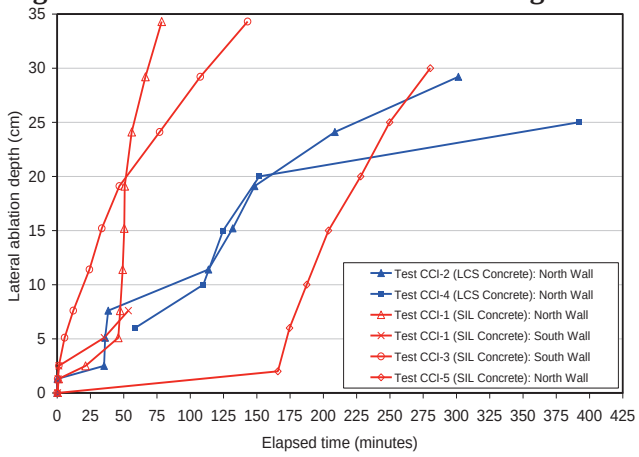

Figure 5. Lateral Ablation for Late Flooding Tests.

Relatively low heat transfer rates to the concrete boundaries were evidenced by the low ablation rates exhibited over the first 40 minutes. Note that this type of behavior is consistent with other transient core oxide tests carried out at Sandia [14], wherein large mass (200 kg) sub-stoichiometric melts consisting of $(U,Zr)O_{2-x}$ were poured into concrete test sections and allowed to cool with no further heating. In these tests, no concrete ablation occurred and the conclusion was drawn that crusts acted to thermally protect the concrete. However, in the current tests the melts were continuously heated. Thus, once the surface crusts failed in CCI-1, ablation proceeded vigorously and the melt temperature fell rapidly in comparison to the other tests. This initial stable crust behavior may have been linked to the exceptionally low gas content for this concrete type in comparison to others used in the test series [1,3]. In particular, gas sparging at the core-concrete interface may provide the mechanical force required to dislodge the crust material from the interface, thereby allowing ablation to proceed. If this is correct, then the reduced gas sparging allowed the insulating crusts to remain stable over an extended period of time in Test CCI-1, which in turn allowed the melt temperature to increase.

Aside from CCI-1, examination of Figs. 4-5 indicates that the other tests also showed evidence of early crust formation phases that influenced the overall ablation behavior. For CCI-2, both axial and lateral ablation rates were initially quite low and the melt temperature relatively constant until ~ 30 minutes, after which time a period of rapid erosion occurred. However, unlike CCI-1, these erosion bursts were not sustained. Rather, after ~ 5 cm of ablation both the axial and lateral ablation rates slowed significantly and approached quasi-steady states. The reduced period of crust stability for CCI-2 is consistent with the idea that gas sparging can disrupt surface crusts, since the gas content of the CCI-2 concrete was significantly greater compared to CCI-1.

Unlike CCI-1 and CCI-2, sidewall erosion in CCI-3 commenced immediately upon contact with melt, and progressed steadily throughout the balance of the test. Conversely, the data suggests that the concrete basemat was protected by an insulating crust until ~ 50 minutes, at which point the crust failed and erosion commenced, albeit at a reduced rate relative to lateral ablation. In contrast, the results of CCI-5 suggest that the sidewall was protected by crust material for nearly 2.5 hours before ablation was initiated. However, once erosion began, the lateral ablation rate approached that observed in CCI-3.

Aside from initial crusting effects, examination of Figs. 4-5 indicates that the long-term ablation process is influenced by concrete type. In particular, long-term lateral and axial ablation rates for Tests CCI-2 and CCI-4, both of which were conducted with LCS concrete, were about the same. For CCI-2, the concrete erosion rate averaged 4 cm/hr over several hours of interaction before gradually decreasing. For CCI-4, the rate was slightly lower, but this is due to a surface scaling effect as the initial cavity size and therefore input power level were reduced to expand the test duration. Thus, the lateral/axial heat flux ratios for these LCS tests are approximately unity.

The relatively uniform power splits for CCI-2 and CCI-4 can be contrasted with the tests conducted with siliceous concrete. In contrast to CCI-1, the other two tests conducted with siliceous concrete (CCI-3 and CCI-5) seemed to exhibit repeatable, albeit non-isotropic, ablation behavior. For CCI-3, fairly symmetrical sidewall ablation occurred. However, unlike Test CCI-2, the lateral ablation was highly pronounced in comparison to axial for this particular test. A similar trend was noted for CCI-5 that was conducted with a single siliceous concrete sidewall. Lateral ablation averaged 10 cm/hr during the late phases of the CCI-3 and CCI-5 experiments, while the axial ablation rate was limited to 2.1 to 2.5 cm/hr over the same timeframe for the two tests. On this basis, the lateral/axial surface heat flux ratios for CCI-3 and CCI-5 were estimated as ~ 4 and ~ 4.7, respectively. These values are significantly higher than the near-unity ratios deduced for tests CCI-2 and CCI-4 with LCS concrete. Thus, the data suggests that there is an effect of concrete type on the spatial heat flux distribution at the core-concrete interface during dry CCI. Similar trends have been observed in tests conducted at CEA [19]. Regarding possible explanations, differences in the two concrete types include: i) chemical composition (viz. LCS concrete

has a high CaO/SiO_2 relative to siliceous), and ii) concrete gas content (LCS has ~ 2.5 times as much gas as siliceous). A third possible explanation was revealed during posttest examinations. In particular, the nature of the core-concrete interface was noticeably different for Test CCI-2 in comparison to Tests CCI-1, CCI-3, and CCI-5, as shown in Fig. 6. The ablation front for the siliceous tests consisted of a region where the core oxide had locally displaced the cement that bonded the aggregate. Conversely, the ablation front for Test CCI-2 consisted of a powdery interface in which the core and concrete oxides were clearly separated. These interfacial characteristics may have influenced the ablation behavior.

Finally, one of the key objectives for CCI-5 was to examine the influence of melt pool aspect ratio on the radial/axial power split under dry cavity conditions. The approach was to increase the test section aspect ratio (i.e., test section width/melt depth) to the greatest extent possible to more accurately mock up prototypic conditions. As discussed in Section 2, the measures that were taken allowed the aspect ratio to be increased from a value of ~ 1 for CCI-3 to ~ 3.2 for CCI-5. The relatively close agreement in long-term ablation behavior for tests CCI-3 and CCI-5 indicate that aspect ratio has little influence on ablation characteristics. This observation lends credibility to the measured power split for siliceous concrete insofar as extrapolating the results to plant conditions.

CCI-1 (SIL)

CCI-3 (SIL)

CCI-5 (SIL)

CCI-2 (LCS)

Figure 6. Axial Debris Morphology for Various Tests (All flooded except CCI-5).

Aside from the overall cavity erosion behavior, video footage from the tests indicated that a crust was present over the melt upper surface during a large fraction of dry cavity ablation phase for all five tests. The crusts contained vent openings which allowed melt eruptions to occur as the tests progressed. The frequency and intensity of the eruptions were directly correlated to the gas content of the concrete for any given test.

In terms of the chemical analyses conducted as part of the test series, samples were collected to: i) characterize the lateral and axial composition variations of the solidified debris, and ii) characterize the composition of corium regions that played key roles in the coolability aspects of the tests (e.g., porous crust zones formed at the melt/water interface, and the material erupted after cavity flooding in CCI-2).

Analysis of samples taken to characterize the lateral composition variation indicate that for most tests, the corium in the central region of the test section had a higher concentration of core oxides in comparison to samples collected near the two ablating concrete sidewalls. Conversely, samples taken to characterize the axial composition variation over the vertical extent of the solidified corium remaining over the basemat indicate the trend of slightly increasing core oxide concentration as the concrete surface is approached. For all three tests conducted with siliceous concrete, two zones appeared to be present: a heavy monolithic oxide phase immediately over the basemat that was enriched in core oxides, with a second overlying porous, light oxide phase that was enriched in concrete oxides. This axial phase distribution is evident in Fig. 6.

Closely linked to the cavity ablation behavior, the test series also provided data on debris coolability under both early as well as late cavity flooding conditions. In terms of phenomenology, the tests provided data on the bulk cooling, water ingression, melt eruption, and transient crust breach cooling mechanisms that are described in [28]. In addition, Tests CCI-2 and CCI-6 provided data on water ingress at the interface between the core material and concrete sidewalls. This mechanism had been previously identified in the COTELS reactor material test series [26,27]. Principal findings from these tests related to debris coolability are summarized as follows.

The debris-water heat fluxes for the various tests are shown in Fig. 7. The fluxes were high during the five minute interval following cavity flooding for all tests. For the two late-flooded tests conducted with siliceous concrete (i.e. CCI-1 and CCI-3), the initial heat removal rates were close to the Critical Heat Flux (CHF) limitation of ~ 1 MW/m^2 under saturated boiling conditions at atmospheric pressure. Thus, the heat fluxes were indicative of quenching of the upper surface crust that was present as an initial condition for both tests. However, for tests CCI-2 and CCI-6, the upper surfaces were essentially devoid of a surface crust when water was introduced. Thus, the high surface temperatures initiated strong film-boiling heat transfer with surface area augmentation, resulting in cooling transients where the initial water cooling rates exceeded CHF by a factor of three or more. The heat fluxes eventually fell below 1 MW/m^2 after ~ 5 minutes once the surface temperature dropped sufficiently for the water to quench the melt surface. At this time, a stable crust most likely formed at the crust-water interface, thereby terminating the bulk cooling transients

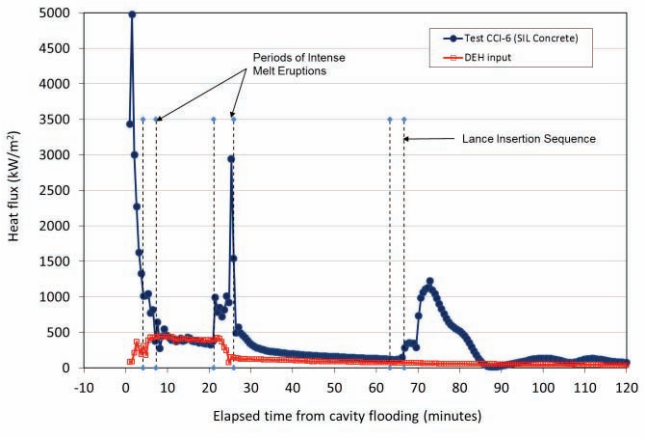

(a)

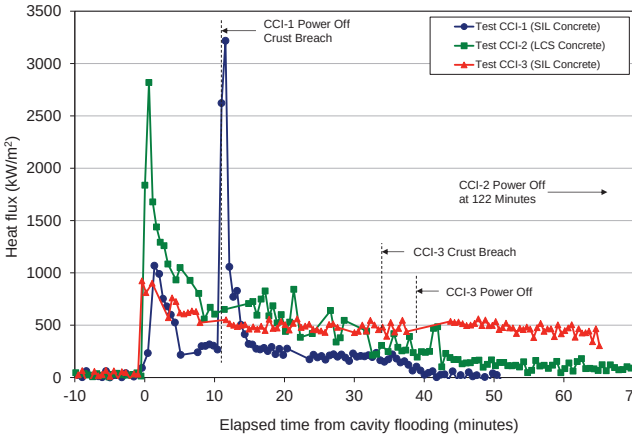

(b)

Figure 7. Debris/Water Heat Flux for (a) Early and (b) Late-Flooded Tests.

The tests did not generally exhibit a decrease in the bulk melt temperature after cavity flooding (Fig. 3). This is despite the fact that the heat flux and power supply responses both indicated substantial debris cooling. This type of behavior can be rationalized by a latent heat transfer process in which a quench front develops at the melt/water interface, as opposed to a sensible heat transfer process in which the entire melt mass is cooled by

convective heat transfer with the heat dissipated to the overlying water by conduction across a thin crust at the melt/water interface. The posttest debris morphologies (Fig. 8) were also consistent with development of quenched debris zones, as opposed to bulk cooldown of the entire melt by conduction-limited cooling across a thin crust.

After the initial transient, the debris/water heat fluxes ranged from 250 to 650 kW/m^2. Heat fluxes for all siliceous concrete tests were lower than the test conducted with LCS concrete. In general, the data indicates that the flux increases with concrete gas content. The heat fluxes realized in these integral effect tests were several times higher than that predicted by the SSWICS water ingression correlation developed as part of the OECD/MCCI program [29]. Thus, the data suggests that the degree of interconnected cracks-fissures-porosity that forms the pathway for water to ingress into solidifying crust material is increased by the presence of gas sparging, particularly for the case in which the melt contains a high concrete fraction. A photograph showing the physical nature of this fractured crust material is shown in Fig. 9.

Aside from the water ingression cooling, the CCI tests also provided data on the melt eruption cooling mechanism in which concrete decomposition gases entrain melt through the crust into overlying water, where the core material is quenched in the form of a porous particle bed. As noted earlier, significant eruptions were observed for Test CCI-2 [28]. Although no spontaneous eruptions were observed in the other two siliceous concrete tests that were flooded late (i.e., CCI-1 to CCI-3), several eruptions were observed in CCI-6 that was flooded essentially at the start of the CCI (Figs. 7-8). Although eruptions were observed in CCI-6, the extent of the eruptions was still larger in the late-flooded LCS test (CCI-2). The primary difference here is the gas content of the concrete used in the two tests (i.e., LCS concrete gas content is ~ 3 times higher than siliceous). A photograph showing the physical characteristics of the particle bed material is provided in Fig. 9.

In terms of the crust breach cooling mechanism, both siliceous concrete tests provided data on *in-situ* crust strength, while CCI-1 also provided data on the extent of cooling after crust breach. The data indicates that crust material formed

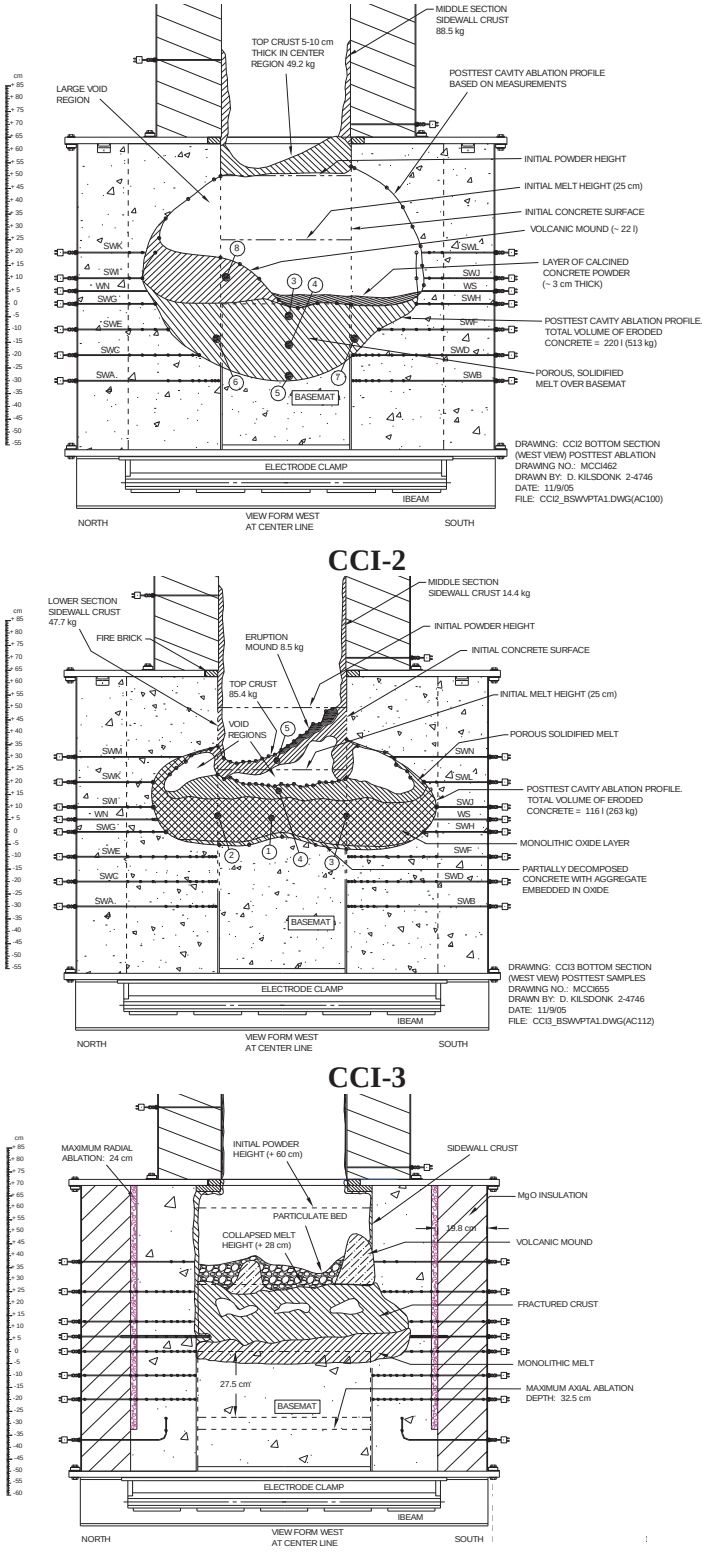

Figure 8. Posttest Debris for CCI Tests.

during quench is very weak, with the inherent crack structure in the material controlling its' overall strength under an applied load. This finding is consistent with the SSWICS test series crust strength measurements [30]. However, the CCI strength measurements were significant because they were carried out under prototypic temperature boundary conditions before the material had cooled to room temperature. Thus, the collection of data from the SSWICS and CCI test series indicates that a floating crust boundary condition is appropriate at plant scale [3], as the material has inadequate strength to support its own weight plus the weight of overlying particle bed and water during core-concrete interaction. This is an important finding as both the water ingression and melt eruption cooling mechanisms required sustained melt-crust contact to proceed and provide, potentially, a pathway to long-term debris coolability under plant accident conditions.

Aside from the strength measurements, the crust breach events in CCI-1 and CCI-6 caused significant transient increases in the debris cooling rate of > 1 MW/m^2 (see Figs. 6-7). After these breaches, the heat flux steadily declined to the levels observed prior to breach. In general, the data indicates that breach events may lead to significant transient increases in the debris cooling rate at plant scale.

Figure 9. Samples of Particle Bed (left) and Fractured Crust (right) Debris Zones Recovered From CCI-6.

Although efficient cooling has been observed for LCS concrete tests under both early as well as late phase flooding conditions, it is noteworthy that the overall cooling behavior for CCI-6 was quite effective relative to the other siliceous concrete tests. This is an important finding for accident management, particularly in light of the fact that the test was conducted with siliceous concrete which has relatively low gas content. The debris-water heat flux, power supply response, and posttest debris morphology for CCI-6 were all consistent with effective cooling [3]. The question arises as to why this test cooled so well relative to previous siliceous concrete tests conducted in the OECD/MCCI and MACE experiment programs [2]. Differences between this experiment and those conducted previously include: i) increased scale, ii) early cavity flooding, iii) lowest initial concrete content in the melt (6 wt %), and iv) *no anchored crust* occurred that confounded coolability demonstration in the MACE experiment program. Finally, another difference between this test and virtually all tests conducted in the MACE program is that CCI-6 utilized a 2-D concrete crucible, as opposed to the 1-D apparatus used in MACE.

Aside from these observations, it is worthwhile to point out a few key elements of the CCI facility that may impact the quenching process observed in the tests. This includes the fact that solidified melt is not heated, as well as the relatively low aspect ratio for the facility that may exaggerate sidewall effects when compared to the reactor case.

3. REMAINING GAPS

As noted in the introduction to this paper, extensive research has been carried out in the area of core-concrete interactions and debris coolability. However, inferences from Fukushima as well as gap analyses carried out after the accident [31] indicate that several areas may warrant additional research. These areas are summarized below:

1) Data for high metal content, reduced power level core debris indicative of BWR systems interacting with concrete under both wet and dry cavity conditions are quite sparse. Dry cavity studies in this area have been carried out at CEA [18]. However, additional work may be warranted under flooded conditions to determine the effect of high metal content on coolability. For example, formation of a metal layer by stratification could impact the water ingression cooling mechanism.
2) Longer-duration testing may be needed to more accurately mock up conditions experienced at Fukushima. The tests that have been conducted have all been less than 8 hours in duration. In addition, extended duration testing would address uncertainties related to transient crust effects observed at the start of many experiments (see discussion in Section 3), the duration of which in several cases is comparable to the overall test duration.
3) Structural concrete in plants contains a large amount of steel (rebar) that can produce additional non-condensable gases during CCI (by reduction of steam to hydrogen). Steel reinforcement may impact coolability; e.g. by changing the concrete macroscopic behavior under thermal loading with the potential for water to ingress along cracks in the concrete. There are ongoing simulant material experiments underway at KIT to investigate the effects of rebar under dry cavity conditions [20], but the reactor material database is quite sparse, particularly for flooded cavity conditions.
4) Finally, for some new reactor designs, provisions have been made to incorporate features that would have a beneficial effect on arresting or considerably slowing down ex-vessel melt progression. However, the efficacy of these features cannot be verified without performance data.

Depending upon the design and accident scenario, there are several additional areas that may warrant additional consideration. This includes deeper melt pools that can form in a cavity with small cross-sectional area, as well as localized accumulations in sumps. In addition, some accident analysis codes predict multiple melt pours following vessel breach; coolability data under these conditions are quite sparse.

4. CONCLUSIONS

Two of the main objectives of the OECD/MCCI Programs were to: 1) resolve the ex-vessel debris coolability issue by providing both confirmatory evidence and test data for coolability mechanisms identified in previous integral effect tests, and 2) address remaining uncertainties related to long-term 2-D core-concrete interaction under both wet and dry cavity conditions. To address these two particular issues, a total of 20 large scale separate- and integral-effect reactor material experiments were carried out. The results of these tests provided both confirmatory evidence and test data to support the development and validation of models that form the technical basis for extrapolating to plant conditions.

In terms of 2-D core-concrete interaction, the experimental approach was to conduct integral effect CCI tests that replicate as close as possible the conditions at plant scale, thereby providing data that can be used to verify and validate the codes directly. To augment the amount of information gathered from these tests, the experiments were flooded from above after a pre-defined concrete ablation depth was reached to provide debris coolability data under conditions involving late phase flooding. The initial input power levels for the tests were selected so that the heat fluxes from the melt to concrete surfaces and the upper atmosphere were initially in the range of that expected early in the accident sequence (i.e., 150-200 kW/m^2). The results of these tests indicate that the power split is a strong function of concrete type; i.e, the split is approximately unity for LCS concrete, whereas split is significantly larger than unity for SIL concrete.

Regarding debris coolability, the results indicate that the efficacy of the cooling process is also strongly linked to the concrete type. In particular, the data indicates that for core melt interaction with LCS concrete, the efficiency of the cooling process is quite effective under both early and late-phase cavity

flooding conditions. This is principally due to the increased efficiency of the melt eruption cooling mechanism that is driven by the high gas content inherent with LCS concrete. Conversely, the cooling efficiency is reduced for core melt interacting with SIL concrete due to the lower gas content for this concrete type. However, the data indicates that the coolability of core melt interacting with SIL concrete is still effective *under early cavity flooding conditions.* This is an important finding related to severe accident management.

Although extensive research has been carried out in this area, inferences from Fukushima as well as analyses carried out after the accident indicate that several areas may warrant additional research. Namely, data for high metal content, reduced power level core debris indicative of BWR systems interacting with concrete under both wet and dry cavity conditions are quite sparse. In addition, longer-duration testing may be needed to more accurately mock up conditions experienced at Fukushima. Structural concrete in plants contains a large amount of steel (rebar) that can produce additional non-condensable gases during CCI that could potentially impact coolability; data regarding this effect are sparse (particularly for the case of reactor materials interacting with concrete). Finally, for some new reactor designs, provisions have been made to incorporate features that would have a beneficial effect on arresting or considerably slowing down ex-vessel melt progression. However, the efficacy of these features cannot be verified without performance data.

ACKNOWLEDGMENTS

This work was sponsored by the Organization for Economic Cooperation and Development (OECD). Participating countries include Belgium, Czech Republic, Finland, France, Germany, Hungary, Japan, Norway, South Korea, Spain, Sweden, Switzerland, and the United States of America. This support is gratefully acknowledged.

REFERENCES

1. M. T. Farmer, S. Lomperski, D. J. Kilsdonk, and R. W. Aeschlimann, "OECD MCCI Project Final Report," OECD/MCCI-2005-TR06 (2006).
2. M. T. Farmer, D. J. Kilsdonk, and R. W. Aeschlimann, "Corium Coolability under Ex-Vessel Accident Conditions for LWRs," *Nucl. Eng. Tech*., **41**, (2009).
3. M. T. Farmer, S. Lomperski, D. J. Kilsdonk, and R. W. Aeschlimann, "OECD MCCI-2 Project Final Report," OECD/MCCI-2010-TR07 (2010).
4. D. A. Powers, D. A. Dahlgren, J. F. Muir, and W. D. Murfin, "Exploratory Study of Molten Core Material/Concrete Interactions July 1975 – March 1977," SAND77-2042 (1978).
5. D. A. Powers and F. E. Arellano, "Large-Scale, Transient Tests of the Interaction of Molten Steel with Concrete," NUREG/CR-2282 (1982).
6. E. R. Copus et al., "Core-Concrete Interactions using Molten Steel with Zirconium on a Basaltic Basemat: The SURC-4 Experiment," NUREG/CR-4994 (1989).
7. E. R. Copus et al., "Experimental Results of Core-Concrete Interactions Using Molten Steel with Zirconium," NUREG/CR-4794 (1990).
8. W. W. Tarbell, D. R. Bradley, R. E. Blose, J. W. Ross, and D. W. Gilbert, "Sustained Concrete Attack by Low-Temperature, Fragmented Core Debris," NUREG/CR-3024 (1987).
9. H. Alsmeyer, "BETA Experiments in Verification of the WECHSL Code: Experimental Results on the Melt-Concrete Interaction," *Nucl. Eng. and Design*, **103**, p. 115 (1987).
10. H. Alsmeyer, "BETA Experiments on Zirconium Oxidation and Aerosol Release During Molten Corium/Concrete Interaction," *2nd CSNI Specialists Meeting on Core Debris-Concrete Interactions*, OECD/NEA/CSNI R(92)10, Karlsruhe, Germany (1992).

11. T. Sevón et al. “HECLA Experiments on Melt–Concrete Interactions: Final Report,” VTT Research Report VTT-R-08013-09 (2009).
12. D. H. Thompson et al., “Thermal-hydraulic Aspects of the Large-Scale Integral MCCI Tests in the ACE program,” *2nd CSNI Specialists Meeting on Core Debris-Concrete Interactions*, OECD/NEA/CSNI R(92)10, Karlsruhe, Germany (1992).
13. J. K. Fink et al., “Aerosol and Melt Chemistry in the ACE Molten Core-Concrete Interaction Experiments,” *High Temperature and Materials Science*, **33**, p. 51 (1995).
14. J. E. Gronager, A. J. Suo-Anttila, and J. E. Brockman, “TURC2 and 3: Large Scale $UO_2/ZrO_2/Zr$ Melt-Concrete Interaction Experiments and Analysis,” NUREG/CR-4521 (1986).
15. E. R. Copus, “Sustained Uranium Dioxide/Concrete Interaction Tests: The SURC Test Series,” *2nd CSNI Specialists Meeting on Core Debris-Concrete Interactions*, OECD/NEA/CSNI R(92)10, Karlsruhe, Germany (1992).
16. E. R. Copus et al., “Core-Concrete Interactions Using Molten Urania with Zirconium on a Limestone-Common Sand Concrete Basemat – The SURC-1 Experiment,” NUREG/CR-5443 (1992).
17. E. R. Copus et al., “Core-Concrete Interactions Using Molten Urania with Zirconium on a Basaltic Basemat – The SURC-2 Experiment,” NUREG/CR-5564 (1992).
18. C. Journeau et al., “Oxide-Metal Corium-Concrete Interaction Test in the VULCANO Facility,” *Proceedings ICAPP ’07*, Nice, France, May 13-18 (2007).
19. C. Journeau et al., “Two-dimensional Interaction of Oxidic Corium with Concretes: The VULCANO VB Test Series,” *Annals of Nuclear Energy*, **36**, p. 1597 (2009).
20. J. J. Foit, T. Cron, B. Fluhrer, A. Miassoedov, and T. Wenz, “MOCKA Experiments on Concrete Erosion by a Metal and Oxide Melt,” ERMSAR-2012, Cologne, Germany (2012).
21. T. G. Theofanous, C. Liu, and W. W. Yuen, “Coolability and Quench of Corium-Concrete Interactions by Top-Flooding,” MACE-TR-D14 (1998).
22. R. E. Blose, J. E. Gronager, A. J. Suo-Anttila, and J. E. Brockman, "SWISS: Sustained Heated Metallic Melt/Concrete Interactions With Overlying Water Pools," NUREG/CR-4727 (1987).
23. R. E. Blose et al., “Core-Concrete Interactions with Overlying Water Pools - The WETCOR-1 Test,” NUREG/CR-5907 (1993).
24. G. Sdouz et al., “The COMET-L2 Experiment on Long-Term MCCI with Steel Melt,” FZKA 7214 (2006).
25. H. Alsmeyer et al., “The COMET-L3 Experiment on Long-Term Melt-Concrete Interaction and Cooling by Surface Flooding,” FZKA 7244 (2007).
26. H. Nagasaka et al., “COTELS Project (1): Overview of Project to Study FCI and MCCI during a Severe Accident,” *OECD Workshop on Ex-Vessel Debris Coolability*, Karlsruhe, Germany (1999).
27. H. Nagasaka et al., “COTELS Project (3): Ex-vessel Debris Cooling Tests,” *OECD Workshop on Ex-Vessel Debris Coolability*, Karlsruhe, Germany (1999).
28. M. T. Farmer et al., “A Summary of Findings from the Melt Coolability and Concrete Interaction (MCCI) Program,” *Proceedings ICAPP ’07*, Nice, France, May 13-18 (2007).
29. S. Lomperski and M. T. Farmer, “Experimental Evaluation of the Water Ingression Mechanism for Corium Cooling,” *Nuclear Eng. Design*, **237**, p. 905 (2006).
30. S. Lomperski and M. T. Farmer, “Corium Crust Strength Measurements,” *Nuclear Eng. Design*, **239**, p. 2551 (2009).
31. R. Bunt, M. Corradini, P. Ellison, M. Farmer, M. Francis5, J. Gabor, R. Gauntt, C. Henry, R. Linthicum, W. Luangdilok, R. Lutz, C. Paik, M. Plys, C. Rabiti, J. Rempe, K. Robb, and R. Wachowiak, “Reactor Safety Gap Evaluation of Accident Tolerant Components and Severe Accident Analysis,” ANL/NE-15/4 (2015).